



HAL
open science

Defective Transcription/Repair Factor IIIH Recruitment to Specific UV Lesions in Trichothiodystrophy Syndrome

Vanessa Chiganças, Keronninn Lima-Bessa, Anne Stary, Carlos F.M. Menck,
Alain Sarasin

► To cite this version:

Vanessa Chiganças, Keronninn Lima-Bessa, Anne Stary, Carlos F.M. Menck, Alain Sarasin. Defective Transcription/Repair Factor IIIH Recruitment to Specific UV Lesions in Trichothiodystrophy Syndrome. *Cancer Research*, 2008, 68 (15), pp.6074-6083. 10.1158/0008-5472.CAN-07-6695. hal-03680000

HAL Id: hal-03680000

<https://hal.science/hal-03680000>

Submitted on 27 May 2022

HAL is a multi-disciplinary open access archive for the deposit and dissemination of scientific research documents, whether they are published or not. The documents may come from teaching and research institutions in France or abroad, or from public or private research centers.

L'archive ouverte pluridisciplinaire **HAL**, est destinée au dépôt et à la diffusion de documents scientifiques de niveau recherche, publiés ou non, émanant des établissements d'enseignement et de recherche français ou étrangers, des laboratoires publics ou privés.

Defective Transcription/Repair Factor IIH Recruitment to Specific UV Lesions in Trichothiodystrophy Syndrome

Vanessa Chiganças,¹ Keronninn M. Lima-Bessa,² Anne Stary,¹ Carlos F.M. Menck,² and Alain Sarasin¹

¹Laboratory of Genetic Stability and Oncogenesis, Centre National de la Recherche Scientifique, Formation de Recherche en Evolution 2939, Institut Gustave Roussy, Université Paris-Sud, Villejuif, France; and ²DNA Repair Laboratory, Instituto de Ciências Biomédicas 2, Universidade de Sao Paulo, Sao Paulo, Brazil

Abstract

Most trichothiodystrophy (TTD) patients present mutations in the *xeroderma pigmentosum D (XPD)* gene, coding for a subunit of the transcription/repair factor IIH (TFIIH) complex involved in nucleotide excision repair (NER) and transcription. After UV irradiation, most TTD/XPD patients are more severely affected in the NER of cyclobutane pyrimidine dimers (CPD) than of 6-4-photoproducts (6-4PP). The reasons for this differential DNA repair defect are unknown. Here we report the first study of NER in response to CPDs or 6-4PPs separately analyzed in primary fibroblasts. This was done by using heterologous photorepair; recombinant adenovirus vectors carrying photolyases enzymes that repair CPD or 6-4PP specifically by using the energy of light were introduced in different cell lines. The data presented here reveal that some TTD/XPD mutations affect the recruitment of TFIIH specifically to CPDs, but not to 6-4PPs. This deficiency is further confirmed by the inability of TTD/XPD cells to recruit, specifically for CPDs, NER factors that arrive in a TFIIH-dependent manner later in the NER pathway. For 6-4PPs, we show that TFIIH complexes carrying an NH₂-terminal XPD mutated protein are also deficient in recruitment of NER proteins downstream of TFIIH. Treatment with the histone deacetylase inhibitor trichostatin A allows the recovery of TFIIH recruitment to CPDs in the studied TTD cells and, for COOH-terminal XPD mutations, increases the repair synthesis and survival after UV, suggesting that this defect can be partially related with accessibility of DNA damage in closed chromatin regions. [Cancer Res 2008;68(15):6074–83]

Introduction

UV light irradiation (UV-C, 254 nm) generates cyclobutane pyrimidine dimers (CPD) and pyrimidine 6-4 pyrimidone photoproducts (6-4PP) as main photolesions in the DNA (1, 2). CPDs correspond to ~75% of these two photoproducts; they produce less significant distortions of the DNA double helix than 6-4PPs and they are generated more often within nucleosomal protected regions (3, 4). Besides, CPDs are repaired more slowly; <50% of CPDs are repaired in 4 hours in the genome overall, in contrast to almost 100% of 6-4PPs removal in the same period of time (4).

Note: Supplementary data for this article are available at Cancer Research Online (<http://cancerres.aacrjournals.org/>).

Requests for reprints: Alain Sarasin, Centre National de la Recherche Scientifique, Formation de Recherche en Evolution 2939, Institut Gustave Roussy, 39 rue Camille Desmoulins, 94805 Villejuif, France. Phone: 33-1-42-11-63-34; Fax: 33-1-42-11-50-08. E-mail: vchiganças@gmail.com or sarasin@igr.fr.

©2008 American Association for Cancer Research.
doi:10.1158/0008-5472.CAN-07-6695

Altogether, these data indicate that CPDs are the most persistent and important players in sensing UV damage in the genome. In fact, CPDs were shown to be a more harmful photoproduct in cells exposed to UV when compared with 6-4PPs (5, 6), and they represent the first signal to UV-induced apoptosis (7, 8).

Nucleotide excision repair (NER) is a highly conserved DNA repair mechanism that is able to remove a variety of bulky DNA lesions such as the UV-induced photoproducts (9). The NER subpathway global genomic repair removes lesions in the entire genome; it is initiated when the xeroderma pigmentosum C (XPC) protein, together with hHR23B, recognizes and binds the helix distortions introduced into DNA by bulky lesions. Thereafter the transcription/repair factor IIH (TFIIH) is recruited to carry strand separation mediated by its two subunits, XPB and XPD, allowing the recruitment of the XPA protein. Incision on each side of the lesion is done by the endonuclease activity of XPG and XPF-ERCC1 leading to excision of the damaged oligonucleotide. The generated gap is filled in using normal replication factors (10).

Trichothiodystrophy (TTD) is a rare human hereditary disease caused by a deficiency in NER and transcription. As a consequence, TTD patients show photosensitivity, skin changes (ichthyosis), and developmental abnormalities such as skeletal defects and neurologic impairment (11). Cells from these patients present mutations in the *XPB*, *XPD*, or *TTD-A (TFB5/p8)* genes, coding for TFIIH subunits (12). The *XPB* and *XPD* genes code for 3'-5' and 5'-3' ATP-dependent helicases, respectively (13), and p8/TTD-A for a recently identified subunit, which stabilizes the entire TFIIH complex (14). One striking characteristic of this syndrome is the reduced intracellular level of TFIIH (15). Moreover, most protein alterations found in these patients change the architecture of the TFIIH complex and, in some cases, can impair its interaction with other transcription factors (16, 17).

Most *XPD* mutations causing TTD are in the COOH-terminal region of the protein, and for these patients the NER of CPDs is always more severely affected than the NER of 6-4PPs (18, 19). A subset of TTD patients show an association with a hotspot change in the NH₂-terminal part of the XPD protein and exhibit an almost complete NER deficiency for both lesions (20–22). The reason why most *XPD* mutations that affect TFIIH are able to decrease much more the repair of CPDs than that of 6-4PPs, when the same factor is responsible for NER for the two lesions, is still on debate. To understand this differential DNA repair defect, we established a system to study the recruitment of NER factors to locally UV-irradiated sites containing specifically only CPDs or only 6-4PPs. We were able to perform this study in physiologic conditions by using an exogenous photorepair pathway. Photorepair is done by enzymes of the photolyase/blue light receptor family; they are lesion specific (CPD-photolyases or 6-4PP-photolyases) and use energy from visible light to split pyrimidine dimers (23).

Our experiments reveal that *XPD* mutations causing TTD syndrome drastically impair the recruitment of TFIIH by XPC-hHR23B in locally irradiated sites only in response to CPDs, whereas they occur normally for 6-4PPs. Complementation with the wild-type (wt) cDNA of the *XPD* gene or treatment with an inhibitor of histone deacetylases, trichostatin A (TSA; ref. 24), restores the recruitment of TFIIH to CPDs. For TFIIH carrying a COOH-terminal mutated XPD, TSA treatment also increases TFIIH-dependent XPA recruitment to the UV-damaged chromatin, NER synthesis, and cell survival for low UV damage conditions. For NH₂-terminal *XPD* mutations in TTD/*XPD* cells, even with recruitment of TFIIH to the 6-4PP lesions, the NER cascade is interrupted between TFIIH and XPA. Our data suggest that *XPD* mutations that confer the TTD phenotype impair the access of TFIIH to lesions within nucleosomes. These new results can help us to understand the repair assembly in relation to different photoproducts and chromatin regions.

Materials and Methods

Cell culture. The cells were grown as described (25). The human primary cells used in this work, 405VI (normal), TTD1VI (*XPD* mutated), TTD9VI (*XPD* mutated), the *XPD*-complemented TTD1VI and TTD9VI, XP22VI (*XPD* mutated), and SV40-TTD1VI, were from our laboratory (26, 27). EBV-based p205-KMT11 plasmid carrying the SV40 large T antigen was used to transform TTD9VI cells (28). The normal SV40-MRC5 transformed cells were from A. Lehmann's laboratory (University of Sussex, Brighton, United Kingdom).

Infection with recombinant adenovirus vectors carrying photolyases. Primary fibroblasts in coverslips were infected with two different purified adenoviruses: one carrying a CPD-photolyase from marsupial (rat kangaroo, *Potorous tridactylus*) as a fusion protein with the reporter protein EGFP (CPD-photolyase-EGFP, vector AdCPDpfr; ref. 25), and a second one carrying a 6-4PP-photolyase from plant (*Arabidopsis thaliana*) coexpressed with EGFP (6-4PP-photolyase-IRES-EGFP, vector Ad6-4pfr; ref. 29). The cells were infected as described (25).

Local UV irradiation and exposure to photoreactivating light. Different cell lines plated on coverslips and treated with different adenovirus were submitted to local UV irradiation (UV-C, 254 nm) as described (30). Photoreactivation was done as described (25). For treatment with TSA (Sigma Aldrich), the inhibitor was added to the medium at a concentration of 10 ng/mL during the photoreactivating light (PRL) incubation.

Immunofluorescence analysis. After the indicated treatments, immunofluorescence was done as described (31). For immunolabeling of CPDs, we used the mouse monoclonal antibody (mAb) TDM-2, and for 6-4PPs the mouse mAb 64M-2 (kindly provided by Dr. T. Mori, Kanazawa University, Kanazawa, Japan; ref. 32); for TFIIH a rabbit polyclonal against XPB (Santa Cruz Biotechnology) and a mouse mAb against the p62 subunit (Euro-medex); for XPA a polyclonal rabbit and for ERCC1 a mouse mAb (Santa Cruz Biotechnology); for XPF a rabbit polyclonal (kindly provided by Dr. J.H.J. Hoeijmakers, Rotterdam, the Netherlands) and for XPC a mouse mAb (kindly provided by Dr. Jaime Angulo, CEA Fontenay aux Roses, France). Secondary antibodies used were Alexa Fluor 350 for analysis in blue color and Alexa Fluor 594 for red (Invitrogen). The slides were analyzed under an immunofluorescence microscope (Olympus PROVIS AX70) with a 100× objective (Olympus UPlanFI 1.3 Oil Iris).

Immunoprecipitation. One hour after UV irradiation, whole-cell extracts of proteins were extracted after scraping from five 100-mm Petri dishes for each treatment point for 20 min under agitation in radioimmunoprecipitation assay buffer (RIPA) buffer [Triton X-10 0.5%, Tris-HCl 50 mmol/L (pH 7.5), EDTA 1 mmol/L, NaCl 50 mmol/L, phenylmethylsulfonyl fluoride 0.2 mmol/L, protease inhibitors] containing benzamide (Novagen) to discard the interference of DNA in the observed protein interactions in response to DNA damage. Four milligrams of whole-cell extracts for normal and TTD1VI and 5 mg for TTD9VI cells were

immunoprecipitated with a mouse anti-XPB mAb (Euromedex) bound in protein A-agarose beads (GE Healthcare) overnight under agitation at 4°C. After extensive washing with RIPA buffer containing NaCl 150 mmol/L, beads were eluted by boiling in SDS gel sample buffer and proteins were analyzed by Western blot. Protein bands were detected with a rabbit polyclonal anti-XPB (Santa Cruz Biotechnology), mouse mAb anti-XPC (Abcam), and mouse mAb anti-XPF (BD Biosciences), and then visualized with antirabbit or antimouse IgG coupled to horseradish peroxidase using the enhanced chemiluminescence kit (Amersham). For the calculation of the ratios XPC/XPB and XPF/XPB, the bands were quantified with the software GeneTools (Syngene Bio Imaging).

Cell fractionation. All chromatin fractionation experiments are based on previous reports (33).

Unscheduled DNA synthesis. These experiments were done as described (34). The samples infected with adenovirus expressing photolyases were immediately kept in PRL conditions for 1 h after UV exposure. The cells were then incubated in the presence of [methyl-³H]thymidine with or without the addition of TSA 10 ng/mL (Sigma Aldrich) for 6 h. This longer incubation time was used to detect NER of CPDs (22). The cells were fixed and analyzed as described (34).

Cell survival. Normal and TTD-derived primary fibroblasts infected with the adenoviral vectors AdCPDpfr and Ad6-4pfr or mock infected were UV irradiated at the different indicated doses. The cells were immediately kept in the presence or absence of TSA 10 ng/mL (Sigma Aldrich) for 24 h. After this period, the culture medium was replaced without TSA. Ninety-six hours after UV irradiation, the cells were washed in PBS and trypsinized, and the adherent cells counted in Z1 Coulter Particle Counter (Beckman Coulter).

Results

Generation of foci containing only one type of photoproduct after local UV irradiation. We studied the recruitment of NER factors to locally UV-irradiated sites containing specifically only CPDs or only 6-4PPs by using heterologous photorepair in human fibroblasts. Recombinant adenovirus vectors carrying different photolyases were used to transfer these enzymes in normal and TTD cells. Specifically, we used a plant 6-4PP-photolyase coexpressed with the reporter gene EGFP (29) for studying NER only in response to CPDs (Fig. 1A). As represented, after infection the cells are locally UV irradiated and immediately kept under dark or PRL conditions for 1 hour. The heterologous 6-4PP-photolyase was proficient in removing its target lesion in PRL conditions in locally irradiated foci (Fig. 1B). For studying NER only in response to 6-4PPs (Fig. 1C), we used a marsupial CPD-photolyase as a fusion protein with EGFP (25). In Fig. 1D, we can observe that the CPD-photolyase was effective in CPD photorepair in PRL conditions, generating locally UV-irradiated spots containing only 6-4PPs. After PRL exposure, the homogeneous distribution of the CPD-photolyase throughout the nucleus is restored between 1 and 4 hours after local UV (25). In addition, we cannot exclude that the permanence of the CPD photolyase at these sites can be due to the presence of 6-4PP lesions after CPD photorepair because some cross-reactivity between CPD-photolyase and 6-4PP has been reported (35). The high UV dose used (150 J/m²) was necessary to visualize the permanence of 6-4PPs lesions 1 hour after irradiation, mainly in cells proficient in NER of 6-4PPs, because these lesions are produced three to five times less abundantly than CPDs and rapidly repaired (4).

The normal recruitment of TFIIH to CPDs (Fig. 1B) and 6-4PPs (Fig. 1D) was also verified by immunostaining of its two subunits, XPB and p62 (Supplementary Fig. S1; ref. 13). The TFIIH complex was our target in these studies because its subunit, XPD, is altered in the TTD cells studied (see below). These results show that we established the first *in vivo* and physiologic system to generate

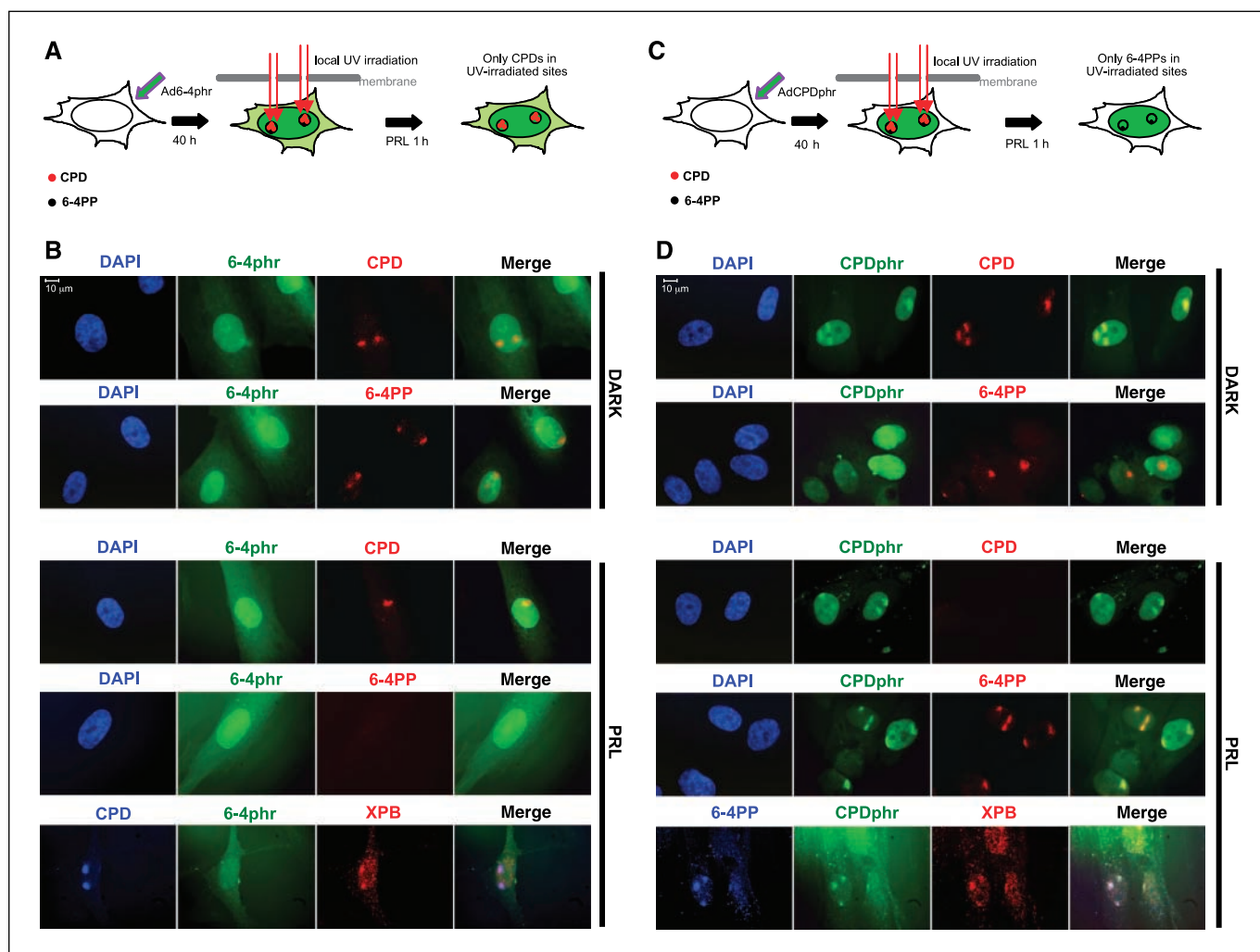


Figure 1. Heterologous photoreactivation in normal human fibroblasts. *A* and *B*, heterologous photorepair of 6-4PPs. *A*, experimental design. CPDs are represented as red dots and 6-4PPs as black dots in locally UV-irradiated sites. *B*, normal fibroblasts were infected with the vector Ad6-4phr, carrying a 6-4PP-photolyase gene from *A. thaliana* coexpressed with the reporter gene GFP (6-4PPphr-IRES-EGFP). Forty hours after infection, the cells were locally UV irradiated at 150 J/m^2 and immediately exposed to dark or PRL conditions for 1 h. Thereafter, the cells were fixed and the presence of CPDs and 6-4PPs was detected by incubation with a mouse CPD-specific mAb (TDM-2) and a mouse 6-4PP-specific mAb (64M-2; ref. 32), respectively, and a subsequent antimouse-Alexa 594. For the analysis of TFIIH, XPB was detected with a rabbit polyclonal antibody in red (Alexa 594) concomitantly with the respective UV lesion in blue (Alexa 350). DAPI, 4',6-diamidino-2-phenylindole. *C* and *D*, heterologous photorepair of CPDs. *C*, experimental design. *D*, normal fibroblasts were infected with the vector AdCPDphr, carrying a marsupial CPD-photolyase as a fusion protein with the reporter gene GFP (CPDphr-EGFP). Forty hours after infection, the cells were treated as described in *B* for the detection of CPD, 6-4PP, and XPB. Representative photos from three independent experiments.

foci containing only a specific UV photoproduct in human diploid fibroblasts.

TFIIH recruitment to CPDs and 6-4PPs after UV in TTD/XPD cells. To understand the NER defects in the TTD syndrome, the recruitment of NER factors to specific UV lesions was investigated as described in Fig. 1. TTD/XPD primary fibroblasts from two TTD patients were used in this work (Fig. 2A). TTD1VI cells have a causal hotspot mutation in the COOH-terminal region of the XPD helicase (R722W) and present a drastic decrease in NER of CPDs in comparison with normal cells, but only a slight delay in NER of 6-4PPs (19, 36). TTD9VI cells are mutated in the hotspot of the NH₂-terminal region of XPD and are deficient in NER for both UV lesions (20–22).

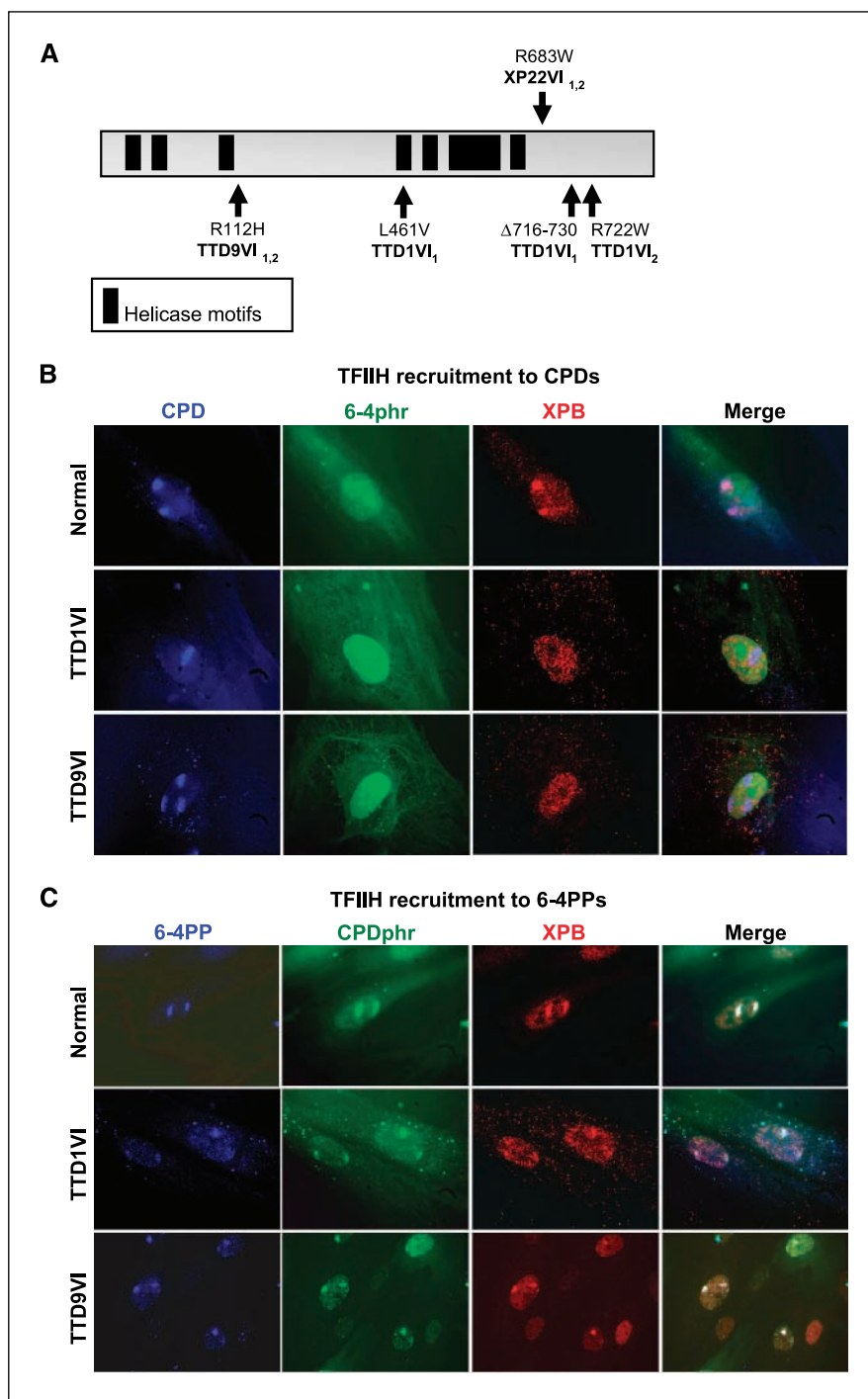
In Fig. 2B, we analyze the recruitment of TFIIH to locally UV-irradiated sites containing only CPDs. The recruitment of XPB to CPDs is observed in NER-proficient cells but is absent for both TTD cells. The same pattern of TFIIH recruitment was also observed for

the p62 factor (Supplementary Fig. S1). This deficiency in recruiting TFIIH to CPDs sites persists at least until 24 hours after UV (Supplementary Fig. S2), suggesting that this observation is not due to a delay but is due to a real failure in recruiting TFIIH to CPDs. Complementation of these TTD cells with the wt *XPD* cDNA recovers DNA repair and cell survival after UV (Supplementary Fig. S3A and B; ref. 27) and restores the recruitment of TFIIH to CPD sites (Supplementary Fig. S3C), confirming the alterations in the XPD protein in these TTD cells as responsible for the impairment in TFIIH recruitment to CPDs.

In contrast, TTD1VI and TTD9VI cells recruit TFIIH to 6-4PPs in locally irradiated spots similarly to normal cells (Fig. 2C), indicating that the studied *XPD* mutations impair the TFIIH recruitment only in response to CPDs.

Analysis of the TFIIH recruitment in foci containing CPDs or 6-4PPs was also done for the XP22VI cell line for comparison. This cell line, isolated from an XP patient, presents a mutation in the

Figure 2. Recruitment of TFIIH complex to locally UV-irradiated sites in normal and TTD cells. **A**, studied mutations in the XPD protein. The TTD1VI cells have three different mutations in the XPD gene; the first allele carry the $XPD^{L461V+del716-730}$, considered with no biological activity from previous experiments done in yeast (50), and the second allele carry the XPD^{R722W} hotspot mutation. The TTD9VI cells are homozygous for the XPD^{R112H} hotspot mutation. The XPD XP22VI cell line is homozygous for the XPD^{R683W} hotspot mutation. **B**, recruitment of TFIIH complex to CPDs. Normal, TTD1VI, and TTD9VI cells were treated as described in Fig. 1A and analyzed in three colors: the presence of CPDs was detected with the TDM-2 antibody in blue (Alexa 350), the expression of the 6-4phr in green, and the TFIIH subunit XPB with a rabbit polyclonal antibody in red (Alexa 594). The merged foci appear in purple. Representative photos from four independent experiments. **C**, recruitment of TFIIH complex to 6-4PPs. Normal, TTD1VI, and TTD9VI cells were treated as described in Fig. 1C; the presence of 6-4PPs was detected with the 64M-2 antibody in blue (Alexa 350; not shown), the expression of the CPDphr in green, and the TFIIH subunit XPB in red. The merged foci appear in orange. Representative photos from four independent experiments.



COOH-terminal region of the XPD gene commonly associated with the XP syndrome, which is observed in at least 70% of XPD patients (Fig. 2A). TFIIH recruitment to locally irradiated sites occurs normally in these XPD cells, no matter if the damaged sites contain only CPDs or only 6-4PPs (Supplementary Fig. S4A), suggesting that only XPD mutations conferring a TTD phenotype impede the TFIIH recruitment specifically to CPDs.

The recruitment of TFIIH to UV lesions occurs specifically by the XPC-hHR23B complex (31). We could not exclude that the impaired TFIIH recruitment observed for TTD cells may represent an indirect consequence of some upstream event. Thus, we also checked

the XPC signal for normal and TTD cells in CPD-containing sites, where no TFIIH is recruited. TTD1VI and TTD9VI are able to recruit XPC to CPDs as NER-proficient cells (Supplementary Fig. S4B), showing that the XPD mutations in these TTD cells affect the recruitment of TFIIH by the XPC-hHR23B complex at CPD sites.

Recruitment of XPA and XPF-ERCC1 for CPDs and 6-4PPs in TTD/XPD cells. After the recruitment of TFIIH by the XPC-hHR23B complex, XPA, replication protein A, XPG, and the XPF-ERCC1 endonuclease complex are the next players in the pathway (31, 37). XPA and XPF-ERCC1 are not observed in CPD-containing sites for TTD1VI and TTD9VI cells (Fig. 3A), adding support to the

data on the impairment in TFIIH recruitment to these sites once the latter is necessary for the continuation of the NER cascade.

We show that XPA and XPF-ERCC1 are recruited normally to 6-4PPs after local UV in NER-proficient and TTD1VI cells (Fig. 3B). However, for TTD9VI cells, deficient also in NER of 6-4PPs, XPA and the XPF-ERCC1 complex fail to relocalize to both lesions CPDs and 6-4PPs (Fig. 3A and B). The complementation of these TTD cells with the wt *XPD* cDNA restores the recruitment of XPA and XPF-ERCC1 to CPD sites for both TTD cell lines, and for the 6-4PP sites in the case of TTD9VI (Fig. 3A and B). These results suggest an interruption in NER between TFIIH and XPA for TTD9VI cells.

Molecular NER responses to CPDs or 6-4PPs in TTD/*XPD* cells. SV40-transformed normal, TTD1VI, and TTD9VI fibroblasts were used for analyzing protein-protein interactions. It is worthy to point out that the failure in TFIIH recruitment only for CPDs site was also observed by immunofluorescence in these SV40-transformed TTD cells when compared with NER-proficient cells, as observed for primary fibroblasts (Supplementary Fig. S5).

It has previously been shown that the recruitment of TFIIH after lesion recognition occurs by the specific affinity of XPC for its subunits XPB and/or p62 (38). For NER-proficient cells (Fig. 4A), we observe an interaction between XPB and XPC after UV irradiation and the consequent XPF recruitment in the pathway. The interactions are reduced in cells expressing the CPD-photolyase and kept under PRL conditions (Fig. 4A, compare lanes 4 and 5) because the CPDs were removed from the genome by the heterologous photolyase; the less abundant 6-4PPs were rapidly removed by the endogenous NER pathway. In contrast, 6-4PP photorepair in normal cells allows the detection of interactions between XPB, XPC, and XPF in response to the remaining CPD lesions in the genome (Fig. 4A, see lane 6).

For TTD1VI cells expressing the 6-4PP-photolyase, we observe impairment in the interaction between XPB and XPC and consequent recruitment of the endonuclease XPF in response specifically to CPDs (Fig. 4B, lane 6). For TTD9VI cells, a defective interaction between XPB and XPC is also observed in response to CPDs (after

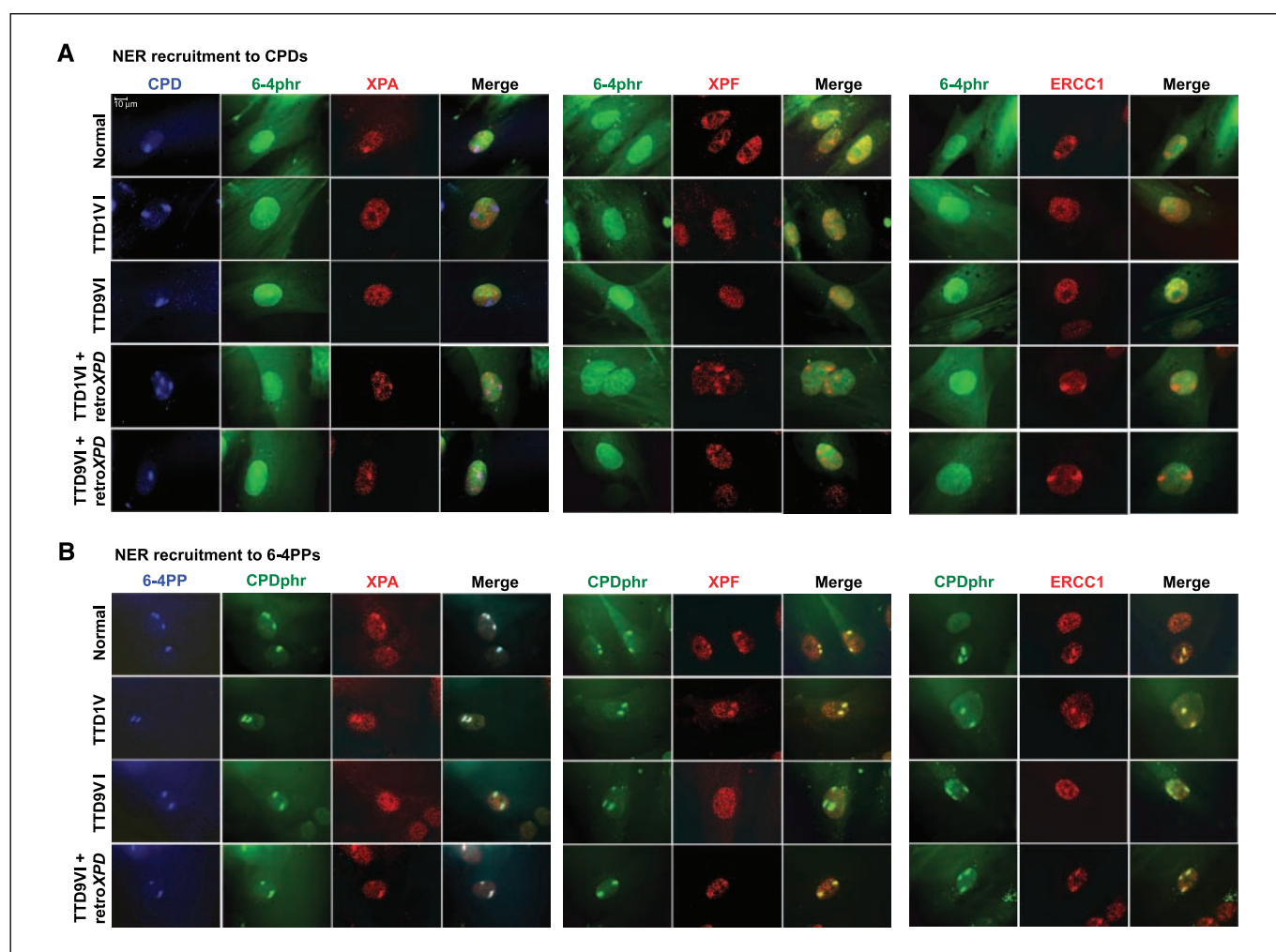


Figure 3. Recruitment of XPA and the XPF-ERCC1 endonuclease complex to UV lesions in normal and TTD cells. **A**, recruitment of XPA and the XPF-ERCC1 endonuclease complex to CPD-containing sites. Normal, TTD1VI, TTD9VI, TTD1VI + retro*XPD*, and TTD9VI + retro*XPD* cells were treated as described in Fig. 1A until the 1-h exposure to PRL. Thereafter, the cells were immediately fixed, and XPA and XPF were detected with rabbit polyclonal antibodies and analyzed in three colors as in Figs. 1 and 2. For the analysis of ERCC1, a mouse anti-ERCC1 antibody was used with a subsequent mouse-Alexa 594 and then counterstained with 4',6-diamidino-2-phenylindole. For simplicity, images of the lesion in blue are shown only for the XPA analysis. The merged foci appear in purple or orange. Representative photos from three independent experiments. **B**, recruitment of XPA and the XPF-ERCC1 endonuclease complex to 6-4PP-containing sites. Normal, TTD1VI, TTD9VI, and TTD9VI + retro*XPD* cells were treated as described in Fig. 1C for the analysis of XPA, XPF, and ERCC1. For simplicity, images of the lesion in blue are shown only for the XPA analysis. The merged foci appear in white or orange. Representative photos from three independent experiments.

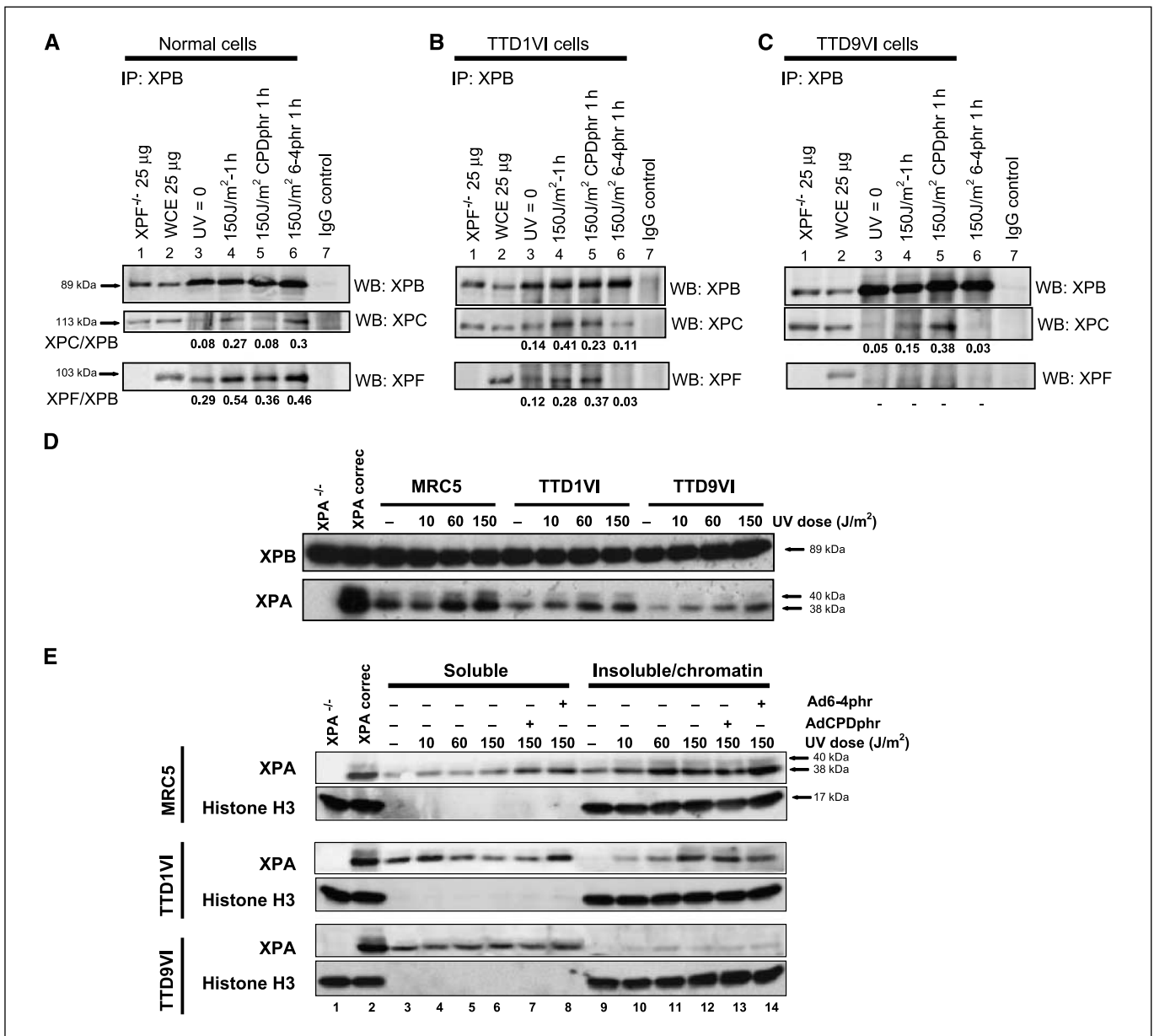


Figure 4. Interaction between NER proteins in SV40-transformed normal and TTD cells. **A to C**, the association of XPB (TFIIH) with XPC and XPF in response to CPDs and 6-4PPs was verified by immunoprecipitation (IP) of XPB in whole-cell extracts (WCE) of the indicated cells. The cells were treated with recombinant adenoviruses carrying photolyases as described in Figs. 1 and 2, and whole-cell extracts were prepared 1 h after global UV irradiation. Immunoprecipitation for MRC5 (**A**; using 4 mg of whole-cell extract), TTD1VI (**B**; 4 mg of whole-cell extract), and TTD9VI cells (**C**; 5 mg of whole-cell extract) was analyzed by Western blot for the detection of XPB, XPC, and XPF. Mutated XPF cells are used as a negative control. The ratios XPC/XPB and XPF/XPB are indicated below the blots following quantification by GeneTools (Syngene Bio Imaging). **D**, XPA increase in nuclear extracts after global UV irradiation in normal and TTD-derived fibroblasts. The cells were irradiated at the indicated UV doses and nuclear extracts were produced after 1 h. Twenty-five micrograms were used in Western blot analysis for the detection of XPB and XPA. Extracts from the insoluble/chromatin fraction of XPA^{-/-} (XP12RO-SV) and XPA^{-/-} corrected with the wt XPA cDNA were used as a reference for XPA signal. **E**, recruitment of XPA after UV irradiation to the chromatin fraction was studied by cellular fractionation in normal and TTD cells as indicated. The signal for histone H3 was used as a control of insoluble/chromatin fraction. **A to E**, blots are representative of three independent experiments.

6-4PP photorepair; Fig. 4C, lane 6). XPB-XPC interaction is still observed when these cells have only 6-4PPs in their genome (after CPD photorepair; Fig. 4C, lane 5). XPF endonuclease fails to be immunoprecipitated with XPB in response to both lesions CPDs and 6-4PPs, reinforcing our observations by immunofluorescence for TTD9VI cells. For TTD cells complemented with the wt XPD cDNA, the pattern of NER interactions is comparable to that of NER-proficient cells (Supplementary Fig. S6). A more complete quantification of the efficiency of coimmunoprecipitation of XPB,

XPC, and XPF is shown in Supplementary Table S1. We indeed confirm that the ability to detect immunoprecipitated complexes between XPC, XPF, and XPB in TTD cells is higher in response to 6-4PPs when compared with NER-proficient cells.

The behavior of XPA after UV irradiation was also analyzed in normal and TTD cells. Confirming previous observations, analysis in nuclear extracts reveals that the XPA protein migrates at two distinct bands at the positions of ~38 and ~40 kDa (Fig. 4D; ref. 39) and accumulates in the nucleus after UV in a

dose-dependent manner for the three cell lines studied (40). TTD cells present less XPA in comparison with normal cells; this can be explained by the severe transcriptional problem characteristic of this syndrome (15).

In cell fractionation, normal cells present maximal recruitment of the XPA protein to chromatin after 60 J/m² UV irradiation (Fig. 4E, lane 11 for MRC5). For TTD1VI cells, this occurs only at a higher UV dose (compare lanes 11 and 12 for MRC5 and TTD1VI cells in Fig. 4E). In these cells, the recruitment of XPA to the chromatin seems to occur essentially by the presence of 6-4PPs when one compares lane 12 (only 150 J/m²) and lane 13 (150 J/m² and CPD photorepair) for TTD1VI cells. These observations are in agreement with the results presented above; TFIIH complexes carrying COOH-terminal mutated XPD are able to recruit the XPA protein, but only in response to 6-4PPs. In contrast, for TTD9VI cells, presenting a XPD NH₂-terminal mutation, no XPA is detected in the insoluble fraction after UV in the presence of either only CPDs or only 6-4PPs (Fig. 4E, lanes 10–14 for TTD9VI cells).

Treatment with TSA restores the TFIIH recruitment to CPDs in TTD cells. Because CPD lesions are more often generated in nucleosomal regions, we verified whether the TFIIH complex carrying *XPD* mutations conferring TTD phenotype could access CPD sites when the chromatin structure is modified (e.g., in conditions of accumulation of acetylated histones; refs. 24, 41). TTD1VI and TTD9VI cells expressing the 6-4PP-photolyase were treated as described in Fig. 1A, locally UV irradiated, and kept under PRL conditions for 1 hour in the presence of 10 ng/mL TSA. In Fig. 5A, we can observe that TSA treatment restores the TFIIH recruitment to CPDs in TTD1VI and TTD9VI cells as good as following the complementation with the wt *XPD* cDNA (compare Supplementary Figs. S3C and S5A).

In addition, the recruitment of XPA to the chromatin fraction in TTD1VI cells after UV irradiation with the UV doses of 10 and 60 J/m² is increased after TSA treatment in comparison with nontreated cells (Fig. 5B, compare lanes 10 and 11 with lanes 13 and 14 for TTD1VI), but not for TTD9VI cells. We believe that a more open chromatin can allow TFIIH complexes mutated in TTD cells to access CPDs and, in the case of the *XPD* COOH-terminal mutation in TTD1VI cells, to recruit XPA.

The DNA repair efficiency (unscheduled DNA synthesis) was measured for normal and TTD cells after UV irradiation, in the presence of only 6-4PPs or only CPDs as well as in the presence of TSA (Table 1). When CPDs and 6-4PPs are present in the genome of the cells, one can notice the NER deficiency for TTD in comparison with normal cells (lines 2 and 3). Photoreactivation of CPDs does not affect the number of grains of repair synthesis in the TTD in comparison with untreated cells because these cells are not carrying out NER for CPDs (lines 4 and 5). In contrast, the action of the 6-4PP-photolyase (lines 6 and 7) decreases the unscheduled DNA synthesis for normal and TTD1VI cells, whereas for TTD9VI cells unscheduled DNA synthesis does not change. Treatment with TSA increases the repair capacity of TTD1VI cells (compare lines 6 and 7 with lines 8 and 9 for TTD1VI) but has no effect for TTD9VI cells. These results indicate that TFIIH complexes in TTD1VI cells carrying a XPD protein R722W can be proficient in NER of CPDs to some extent if access to these lesions is made in a more open chromatin. In contrast, the *XPD* NH₂-terminal mutation in TTD9VI cells renders the TFIIH complex unable to continue the NER process of CPDs even after accessing the lesion site.

In Fig. 5C, we can observe that 10 ng/mL TSA can also increase the survival of TTD1VI cells, but only after irradiation with a low

UV dose (5 J/m²; Fig. 5C, asterisks). No effect of TSA is observed for normal and TTD9VI cells no matter the UV dose or condition used. Altogether, our data indicate that the differential DNA repair defect in TTD syndrome can be partially explained by an inability to access CPDs within nucleosomal structures.

Discussion

The two main UV-induced photoproducts, CPDs and 6-4PPs, are surely not similarly perceived in the nucleus of UV-irradiated cells. Indeed, they are generated in different amounts; they do not distort the double helix at the same degree; and they are produced in distinct locations of the chromatin (3, 4). Most TTD cell lines are more severely affected in the NER of CPDs in comparison with 6-4PPs, and an explanation for this differential DNA repair defect is still to be found. To better understand the DNA repair defects in TTD patients, we established a system to investigate the recruitment of NER factors to specific UV lesions, CPDs or 6-4PPs, by using heterologous photorepair. To our knowledge, this is the first analysis of recruitment of NER proteins to each UV-induced photoproduct studied separately in locally irradiated sites in living human fibroblasts. Moreover, the use of primary cells from NER-proficient and TTD patients allowed us to determine the behavior of endogenous proteins at physiologic levels.

We show that the recruitment of TFIIH factors carrying the XPD mutated proteins in TTD1VI and TTD9VI cells is drastically impaired specifically to CPDs. By immunostaining and immunoprecipitation, we showed that NER factors that arrive subsequently to TFIIH in the repair pathway are also not properly assembled in response specifically to CPDs for these TTD cells. TFIIH and downstream NER factor recruitments to CPDs are recovered when these TTD cells are complemented with the wt *XPD* cDNA, pointing out that the XPD mutated protein is responsible for the interrupted NER pathway. In contrast, in fibroblasts from a XPD patient, TFIIH is recruited to CPD and 6-4PP-containing sites as in NER-proficient cells. This suggests that *XPD* mutations conferring exclusively a TTD phenotype may impair the TFIIH recruitment specifically to CPD lesions.

TSA treatment can also rescue the TFIIH recruitment to CPDs in the TTD cells studied. Having shown that the XPC recruitment to CPDs is normal for these cells, our data suggest that XPC-hHR23B is able to access CPDs within nucleosomes, but the TFIIH recruitment by XPC cannot take place at these sites, whereas it is normal for 6-4PPs. This means that the *XPD* mutations in TTD1VI and TTD9VI cells do not interfere with the interaction between XPC and TFIIH per se, but the TFIIH carrying the XPD mutated protein cannot interact with XPC, particularly in nucleosomal regions. *XPD* mutations affect the structure of the TFIIH complex, influencing its interaction with other transcription factors (42) and its composition (17). This alteration can be a simple topological impediment when this complex needs to access CPDs within nucleosomes. In addition, we cannot exclude that, after the XPC recruitment to UV lesions, the damaged region still requires ongoing modifications involving chromatin reorganization. It has been shown that the p48/damaged DNA binding (DDB)-2 protein helps XPC recruitment to locally UV-irradiated sites specifically for CPDs (35). Later, other groups have also revealed that before the arrival of the complex XPC-hHR23B to the lesion site, the activities of the UV-DDB complex, together with the E3-ubiquitin ligase Cul-4A in chromatin remodeling, are very important (43, 44), but there are no studies about similar activities downstream of XPC during NER. Experiments in yeast (45) and human cells (46, 47) show an increase in

the levels of histone acetylation after UV and the contribution of this response to NER. We believe that generating an environment of hyperacetylated histones after TSA treatment provides the necessary condition that would probably expose UV lesions and allow the recruitment of the mutated TFIIH complexes in the TTD cells studied.

Interestingly, TSA can restore the TFIIH recruitment to CPDs for both TTD cells studied, but only for TTD1VI cells can we observe an effect also downstream of TFIIH, such as XPA recruitment to chromatin, repair synthesis, and cell survival. *In vitro* analyses using TFIIH reconstituted with several purified XPD mutated proteins (17) revealed some specific deficiencies for TFIIH complexes carrying XPD R112H (TTD9VI) or XPD R722W (TTD1VI). Studies with TFIIH carrying XPD R112H detect no helicase activity and no NER synthesis. In comparison, TFIIH complexes carrying XPD R722W are also deficient for helicase activity, but a residual activity can still be detected, and these complexes can perform low but significant levels of NER. This residual helicase and, consequently, the NER activity for TFIIH complexes carrying XPD R722W may explain the fact that TSA treatment allows these complexes to recruit XPA and perform NER synthesis to some extent. For low UV irradiation conditions, this partial TSA-induced recovery in NER can also increase cell survival.

The TFIIH recruitment for 6-4PPs occurs normally in the TTD cells studied. Even for TTD9VI cells, which are unable to remove 6-4PPs from the genome after UV, the NER cascade is intact at least until TFIIH. However, XPA and XPF-ERCC1 factors fail to relocate to 6-4PP-containing sites. Immunoprecipitation and cell fractionation studies in TTD9VI cells confirm a defective recruitment of XPA to chromatin and of XPF-ERCC1 to NER complexes in response to 6-4PPs. Interestingly, cells from TTD-A patients, mutated in the TFIIH subunit p8, are also unable to recruit XPA in locally UV-irradiated sites (48). It is possible that the NH₂-terminal mutation in TTD9VI cells may impair the interaction between XPD and p8 (14, 49). The connection of XPD with the complex p52/XPB mediated by p8 is probably crucial for the proper opening of the damaged DNA and consequent repositioning of XPC and recruitment of XPA (49). Together with our presented data, this may explain why TTD9VI cells with *XPD* mutations in the NH₂ terminus, even with TFIIH recruitment, are unable to perform NER of 6-4PPs.

To summarize, we propose that *XPD/TTD* mutations impair the entry of TFIIH complex specifically in nucleosomal sites containing CPDs, partially explaining the DNA repair defect for this syndrome. Specifically for the NER of 6-4PPs, COOH-terminal mutations, such as the R722W in TTD1VI cells, still allow for TFIIH-mediated XPA recruitment in the lesion site and continuation of the NER

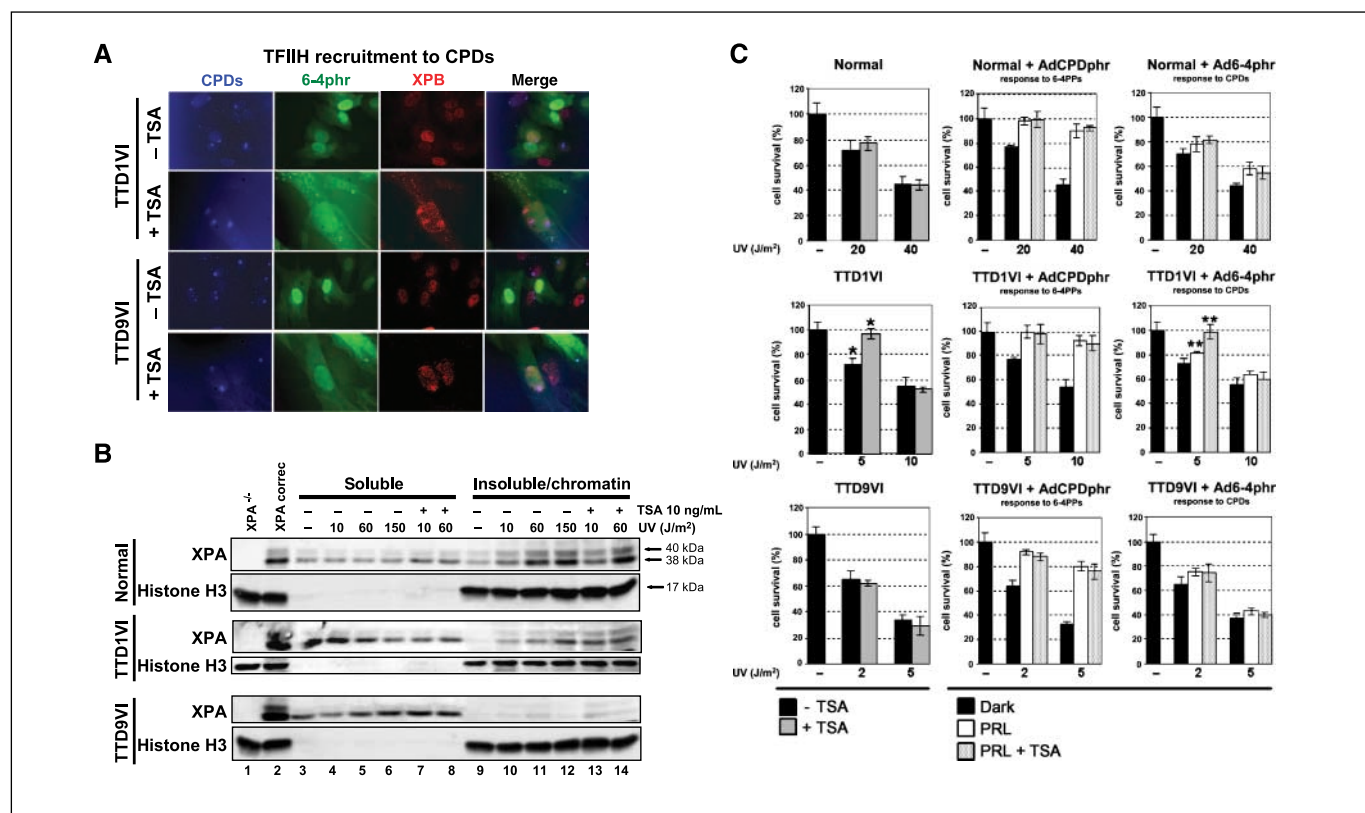


Figure 5. Effect of TSA on NER and cell survival after UV in normal and TTD cells. **A**, recruitment of TFIIH complex to CPDs in TTD primary fibroblasts treated or not with TSA. TTD1VI and TTD9VI cells were treated as described in Fig. 1A until local UV irradiation. Thereafter, the cells were kept for 1 h under PRL conditions in medium containing 10 ng/mL TSA. The cells were then immediately fixed and the slides analyzed in three colors as described in Figs. 1 and 2. The merged foci appear in orange. Representative photos from two independent experiments. **B**, recruitment of XPA to the chromatin fraction was studied by cellular fractionation in SV40-transformed normal and TTD cells treated or not with 10 ng/mL TSA for 1 h after global UV irradiation. Extracts from the insoluble/chromatin fraction of XPA^{-/-} (XP12RO-SV) and XPA^{-/-} corrected with the wt XPA cDNA were used as a reference for XPA signal. Blots are representative of three independent experiments. **C**, effect of TSA on cell survival after UV. Normal, TTD1VI, and TTD9VI primary fibroblasts were UV irradiated at the indicated doses and, for those samples treated with TSA, 10 ng/mL TSA was added to the culture medium for 24 h. After this period, the culture medium was changed and the cells were kept without TSA. For the photoreactivation experiments, the cells were kept for 1 h under PRL conditions immediately after UV, and then 10 ng/mL TSA was added to the medium for 24 h. After this period, their culture medium was replaced as described above. Cell survival was measured as the percentage of adherent cells 96 h after the indicated treatments. Bars, SD (each sample in triplicate, four independent experiments). * and **, $P < 0.01$, Student's *t* test.

Table 1. Measurement of DNA repair synthesis (unscheduled DNA synthesis) in normal and TTD-derived human fibroblasts after UV irradiation

	CPDs	6-4PPs	Treatment	Normal	TTD1VI	TTD9VI
1	—	—	UV 0 J/m ²	0.63 ± 0.15	0.36 ± 0.54	0.56 ± 0.3
2	+	+	UV 5 J/m ²	22.1 ± 2.7	9.2 ± 2.2	3.4 ± 1.4
3	+	+	UV 15 J/m ²	48.5 ± 3.8	10.8 ± 1.9	4.9 ± 2.3
4	PRL	+	UV 5 J/m ²	17 ± 4.5	8.6 ± 2.5	3.9 ± 2
5	PRL	+	UV 15 J/m ²	30.2 ± 3.3	10.8 ± 1.7	4.1 ± 1.9
6	+	PRL	UV 5 J/m ²	11.4 ± 2.7	5.8 ± 2.3*	3.9 ± 1.3
7	+	PRL	UV 15 J/m ²	22.2 ± 3.1	6.8 ± 1.9 [†]	5.6 ± 2
8	+	PRL	UV 5 J/m ² , TSA 10 ng/mL	13 ± 2.5	16 ± 2.3*	4.2 ± 1.9
9	+	PRL	UV 15 J/m ² , TSA 10 ng/mL	24 ± 3.7	20 ± 1.8 [†]	4.5 ± 1.9

NOTE: Normal, TTD1VI, and TTD9VI primary fibroblasts were infected with AdCPDphr or Ad6-4phr, as described in Fig. 1, UV irradiated at the indicated doses, and immediately kept under dark or PRL conditions. Thereafter, DNA repair synthesis was measured by the incorporation of [methyl-³H]thymidine during 6 h in the presence or absence of TSA (10 ng/mL). The grains are counted in 50 different cell nucleus according to ref. 34. —, absence of the indicated lesion in nonirradiated cells (control). +, presence of the indicated lesion after UV treatment. PRL, absence of the indicated lesion after heterologous photorepair (photoreactivation, PRL).

*Statistically significant difference between TSA-treated and nontreated cells for 5 J/m² ($P < 0.01$, Student's *t* test).

[†]Statistically significant difference between TSA-treated and nontreated cells for 15 J/m² ($P < 0.01$, Student's *t* test).

assembly. In contrast, NH₂-terminal mutations, such as the R112H in TTD9VI cells, may affect the p8-mediated connection of XPD with the complex p52/XPB, abolishing the recruitment of XPA.

The causes for this specific defect in TFIIH recruitment to CPDs are still not entirely deciphered. We intend to verify whether this defect is only a passive, topological consequence of conformational changes in the TFIIH complex or whether *XPD* mutations causing TTD may affect the TFIIH structure and function in such a way that some activity required only for CPD sites is lost. These studies can reveal how much the DNA repair activity varies in response to different lesions and regions of the chromatin and can help us to better understand the molecular mechanisms behind DNA repair-related diseases.

Disclosure of Potential Conflicts of Interest

No potential conflicts of interest were disclosed.

References

- de Boer J, Hoesjmakers JH. Nucleotide excision repair and human syndromes. *Carcinogenesis* 2000;21:453–60.
- Vink AA, Roza L. Biological consequences of cyclobutane pyrimidine dimers. *J Photochem Photobiol B* 2001;65:101–4.
- Sage E. Distribution and repair of photolesions in DNA: genetic consequences and the role of sequence context. *Photochem Photobiol* 1993;57:163–74.
- Pfeifer GP. Formation and processing of UV photoproducts: effects of DNA sequence and chromatin environment. *Photochem Photobiol* 1997;65:270–83.
- Marionnet C, Armier J, Sarasin A, Sary A. Cyclobutane pyrimidine dimers are the main mutagenic DNA photoproducts in DNA repair-deficient trichothiodystrophy cells. *Cancer Res* 1998;58:102–8.
- Garinis GA, Mitchell JR, Moorhouse MJ, et al. Transcriptome analysis reveals cyclobutane pyrimidine dimers as a major source of UV-induced DNA breaks. *EMBO J* 2005;16:3952–62.
- Chigaças V, Miyaji EN, Muotri AR, et al. Photorepair prevents ultraviolet-induced apoptosis in human cells expressing the marsupial photolyase gene. *Cancer Res* 2000;60:2458–63.
- Jans J, Schul W, Sert YG, et al. Powerful skin cancer protection by a CPD-photolyase transgene. *Curr Biol* 2005;15:105–15.
- Costa RMA, Chigaças V, Galhardo RS, Carvalho H, Menck CFM. The eukaryotic nucleotide excision repair pathway. *Biochimie* 2003;85:1083–99.
- Friedberg EC, Walker GC, Siede W, Wood RD, Schultz RA, Ellenberger T. DNA repair and mutagenesis. Washington: ASM Press; 2005.
- Itin PH, Sarasin A, Pittelkow MR. Trichothiodystrophy: update on the sulfur-deficient brittle hair syndromes. *J Am Acad Dermatol* 2001;44:891–920.
- Bergmann E, Egly JM. Trichothiodystrophy, a transcription syndrome. *Trends Genet* 2001;17:279–86.
- Frit P, Bergmann E, Egly JM. Transcription factor IIIH: a key player in the cellular response to DNA damage. *Biochimie* 1999;81:27–38.
- Giglia-Mari G, Coin F, Ranish JA, et al. A new, tenth subunit of TFIIH is responsible for the DNA repair syndrome trichothiodystrophy group A. *Nat Genet* 2004;36:714–9.
- Botta E, Nardo T, Lehmann AR, Egly JM, Pedrini AM, Stefanini M. Reduced level of the repair/transcription factor TFIIH in trichothiodystrophy. *Hum Mol Genet* 2002;11:2919–28.
- de Boer J, van Steeg H, Berg RJ, et al. Mouse model for the DNA repair/basal transcription disorder trichothiodystrophy reveals cancer predisposition. *Cancer Res* 1999;59:3489–94.
- Dubaele S, de Santis LP, Bienstock RJ, et al. Basal transcription defect discriminates between xeroderma pigmentosum and trichothiodystrophy in XPD patients. *Mol Cell* 2003;11:1635–46.
- Lehmann AR, Arlett CF, Broughton BC, et al. Trichothiodystrophy, a human DNA repair disorder with heterogeneity in the cellular response to ultraviolet light. *Cancer Res* 1988;48:6090–6.
- Eveno E, Bourre F, Quilliet X, et al. Different removal of ultraviolet photoproducts in genetically related xeroderma pigmentosum and trichothiodystrophy diseases. *Cancer Res* 1995;55:4325–32.
- Broughton BC, Lehmann AR, Harcourt SA, et al. Relationship between pyrimidine dimers, 6-4 photoproducts, repair synthesis and cell survival: studies

Acknowledgments

Received 12/17/2007; revised 5/3/2008; accepted 5/9/2008.

Grant support: K.M. Lima-Bessa and C.F.M. Menck have funds from Fundação de Amparo à Pesquisa do Estado de São Paulo (São Paulo, Brazil), Conselho Nacional de Desenvolvimento Científico e Tecnológico, and Coordenação de Aperfeiçoamento Pessoal de Nível Superior (Brasília, Brazil)-Comitê Francês d'Evaluation de la Coopération Universitaire avec le Brésil [Ministère des Affaires Étrangères (Direction générale de la coopération internationale et du développement) and Ministère de l'Éducation Nationale (Délégation aux relations internationales et de coopération)]. Grants to A. Sarasin have been given by Centre National de la Recherche Scientifique (Paris, France), University Paris XI (Kremlin-Bicêtre, France), Ligue Nationale Contre le Cancer (Paris, France), Association pour la Recherche sur le Cancer (Villejuif, France), and Association Française contre les Myopathies (Evry, France).

The costs of publication of this article were defrayed in part by the payment of page charges. This article must therefore be hereby marked *advertisement* in accordance with 18 U.S.C. Section 1734 solely to indicate this fact.

We thank Odile Chevallier (Institut Gustave Roussy, Villejuif, France) for the complementation of TTD with recombinant retrovirus, Dr. T. Mori for the TDM-2 and 64M-2 antibodies, Dr. Jaime Angulo for the anti-XPC antibody, and Dr. J.H.J. Hoeijmakers for the anti-XPD antibody. V. Chigaças had a 1-year postdoctoral fellowship from the IARC (Lyons, France) and a 2-year postdoctoral fellowship from the Association pour la Recherche sur le Cancer (Villejuif, France).

- using cells from patients with trichothiodystrophy. *Mutat Res* 1990;235:33–40.
21. Berneburg M, Clingen PH, Harcourt SA, et al. The cancer-free phenotype in trichothiodystrophy is unrelated to its repair defect. *Cancer Res* 2000;60:431–8.
 22. Riou L, Eveno E, van Hoffen A, van Zeeland AA, Sarasin A, Mullenders LH. Differential repair of the two major UV-induced photolesions in trichothiodystrophy fibroblasts. *Cancer Res* 2004;64:889–94.
 23. Carell T, Burgdorf T, Mohan K, Cichon M. The mechanism and action of photolyases. *Curr Opin Chem Biol* 2001;5:491–8.
 24. Marks PA, Richon VM, Miller T, Kelly WK. Histone deacetylase inhibitors. *Adv Cancer Res* 2004;91:137–68.
 25. Chiganças V, Sarasin A, Menck CFM. CPD-photolyase adenovirus-mediated gene transfer in normal and DNA-repair-deficient human cells. *J Cell Sci* 2004;117:3579–92.
 26. Marionnet C, Benoit A, Benhamou S, Sarasin A, Stary A. Characteristics of UV-induced mutation spectra in human XP-D/ERCC2 gene-mutated xeroderma pigmentosum and trichothiodystrophy cells. *J Mol Biol* 1995;252:550–62.
 27. Quilliet X, Chevaller-Lagente O, Eveno E, et al. Long-term complementation of DNA repair deficient human primary fibroblasts by retroviral transduction of the XPD gene. *Mutat Res* 1996;64:161–9.
 28. Stary A, Menck CFM, Sarasin A. Description of a new amplifiable shuttle vector for mutagenesis studies in human cells: application to *N*-methyl-*N*'-nitro-*N*-nitrosoguanidine-induced mutation spectrum. *Mutat Res* 1992;272:101–10.
 29. Lima-Bessa KM, Armelini MG, Chiganças V, et al. CPDs and 6-4PPs play different roles in UV-induced cell death in normal and NER-deficient human cells. *DNA Repair (Amst)* 2008;7:303–12.
 30. Mone MJ, Volker M, Nikaido O, et al. Local UV-induced DNA damage in cell nuclei results in local transcription inhibition. *EMBO Rep* 2001;2:1013–7.
 31. Volker M, Mone MJ, Karmakar P, et al. Sequential assembly of the nucleotide excision repair factors *in vivo*. *Mol Cell* 2001;8:213–24.
 32. Mori T, Nakane M, Hattori T, Matsunaga T, Ihara M, Nikaido O. Simultaneous establishment of monoclonal antibodies specific for either cyclobutane pyrimidine dimer or (6-4)photoproduct from the same mouse immunized with ultraviolet-irradiated DNA. *Photochem Photobiol* 1991;54:225–32.
 33. Zou L, Cortez D, Elledge SJ. Regulation of ATR substrate selection by Rad17-dependent loading of Rad9 complexes onto chromatin. *Genes Dev* 2002;16:198–208.
 34. Sarasin A, Blanchet-Bardon C, Renault G, Lehmann AR, Arlett CF, Dumez Y. Prenatal diagnosis in a subset of trichothiodystrophy patients defective in DNA repair. *Br J Dermatol* 1992;127:485–91.
 35. Fitch ME, Nakajima S, Yasui A, Ford JM. *In vivo* recruitment of XPC to UV-induced cyclobutane pyrimidine dimers by the DDB2 gene product. *J Biol Chem* 2003;278:46906–10.
 36. Nishiwaki Y, Kobayashi N, Imoto K, et al. Trichothiodystrophy fibroblasts are deficient in the repair of UV-induced cyclobutane pyrimidine dimers and (6-4) photoproducts. *J Invest Dermatol* 2003;122:526–32.
 37. Riedl T, Hanaoka F, Egly JM. The comings and goings of nucleotide excision repair factors on damaged DNA. *EMBO J* 2003;22:5293–303.
 38. Yokoi M, Masutani C, Maekawa T, Sugawara K, Ohkuma Y, Hanaoka F. The xeroderma pigmentosum group C protein complex XPC-HR23B plays an important role in the recruitment of transcription factor IIIH to damaged DNA. *J Biol Chem* 2000;275:9870–5.
 39. Wu X, Shell SM, Yang Z, Zou Y. Phosphorylation of nucleotide excision repair factor xeroderma pigmentosum group A by ataxia telangiectasia mutated and Rad3-related-dependent checkpoint pathway promotes cell survival in response to UV irradiation. *Cancer Res* 2006;66:2997–3005.
 40. Wu X, Shell SM, Liu Y, Zou Y. ATR-dependent checkpoint modulates XPA nuclear import in response to UV irradiation. *Oncogene* 2007;26:757–64.
 41. Butler LM, Zhou X, Xu WS, et al. The histone deacetylase inhibitor SAHA arrests cancer cell growth, up-regulates thioredoxin-binding protein-2, and down-regulates thioredoxin. *Proc Natl Acad Sci U S A* 2002;99:11700–5.
 42. Keriell A, Stary A, Sarasin A, Rochette-Egly C, Egly JM. XPD mutations prevent TFIIH-dependent transactivation by nuclear receptors and phosphorylation of RAR α . *Cell* 2002;109:125–35.
 43. El-Mahdy MA, Zhu Q, Wang QE, Wani G, Praetorius-Ibba M, Wani AA. Cullin 4A-mediated proteolysis of DDB2 protein at DNA damage sites regulates *in vivo* lesion recognition by XPC. *J Biol Chem* 2006;281:13404–11.
 44. Wang H, Zhai L, Xu J, et al. Histone H3 and H4 ubiquitylation by the CUL4-DDB-ROCI ubiquitin ligase facilitates cellular response to DNA damage. *Mol Cell* 2006;22:383–94.
 45. Yu Y, Teng Y, Liu H, Reed SH, Waters R. UV irradiation stimulates histone acetylation and chromatin remodeling at a repressed yeast locus. *Proc Natl Acad Sci U S A* 2005;102:8650–5.
 46. Wang J, Chin MY, Li G. The novel tumor suppressor p33ING2 enhances nucleotide excision repair via induction of histone H4 acetylation and chromatin relaxation. *Cancer Res* 2006;66:1906–11.
 47. Kuo WH, Wang Y, Wong RP, Campos EI, Li G. The ING1b tumor suppressor facilitates nucleotide excision repair by promoting chromatin accessibility to XPA. *Exp Cell Res* 2007;313:1628–38.
 48. Coin F, de Santis LP, Nardo T, Zlobinskaya O, Stefanini M, Egly JM. p8/TTD-A as a repair-specific TFIIH subunit. *Mol Cell* 2006;21:215–26.
 49. Coin F, Oksenysh V, Egly JM. Distinct roles for the XPB/p52 and XPD/p44 subcomplexes of TFIIH in damaged DNA opening during nucleotide excision repair. *Mol Cell* 2007;26:245–56.
 50. Taylor EM, Broughton BC, Botta E, et al. Xeroderma pigmentosum and trichothiodystrophy are associated with different mutations in the XPD (ERCC2) repair/transcription gene. *Proc Natl Acad Sci U S A* 1997;94:8568–3.